Biomass Decomposition:

A Study on the Effects of Organic Salt Promoted Hydrolysis on Cellulose

A Major Qualifying Project Submitted to the Faculty of

Worcester Polytechnic Institute

In partial fulfillment of the requirements for the

Degree of Bachelor of Science

In

Mechanical Engineering

By:

Katherine Ralph

Advisor:

Michael Timko

Mentor:

Ziyang Zhang

4/20/2021

Table of Contents

Abstract 3

Acknowledgements 4

Chapter 1: Introduction 5

Chapter 2: Background 7

2.1 Lignocellulosic Biomass -Structure and Composition 7

2.2Cellulose 8

2.3 Current Cellulose Hydrolysis Model 8

2.4 Hofmeister Series 9

Chapter 3: Methodology 11

Materials and Methods 11

3.1Materials 11

3.2Methods 11

3.2.1 Ball milling Pretreatment 11

3.2.2 Oil Bath Temperature Calibration 12

3.2.3 Preparing Salt Solutions 12

3.2.4 Salt-Acid Hydrolysis 13

3.2.5 Centrifuge Process and Sample Collection 13

3.3 Characterization 14

3.3.1 X-Ray Diffractometer (XRD) 14

3.3.2 High Performance Liquid Chromatography (HPLC) 15

Chapter 4: Results and Discussion 15

4.1 Cation Effect on Suppression of Cellulose Recrystallization 15

4.2 Anion Effect on Suppression of Cellulose Recrystallization 16

4.3 Glucose Yields of Fixed-Anion Salt Selections 17

4.4 Glucose Yields of Fixed-Cation Salt Selections 18

Chapter 5: Conclusion 20

References 21

Procedures Addendum: 22

Sample Calculations to determine mass for molar solution preparation 24

Abstract

Ongoing research focuses on developing methods to improve the conversion of biomass into biofuels. Traditional mechanical pretreatment like ball-milling increases the cellulose reactivity, but cellulose re-crystallizes in water, making the process ineffective. The goal of the project was to explore Hofmeister series-based salts and analyze the salts' effects on cellulose re-crystallization and subsequent glucose yields post hydrolysis. The experiment was carried out in two parts, the first with a salt selection containing fixed-anions (Cl-), the second with a salt selection containing fixed-cations (Na+). The salts' ability to suppress crystallinity correlates with its performance in glucose yield, showing that the performance of salts agrees with the Hofmeister series. Specifically, salting-in salt such as guanidinium chloride gives highest yield while salting-out salt like ammonium chloride has the lowest glucose yield. The yield differences were attributed to their ability to suppress recrystallization.

Acknowledgements

I would like to thank my advisor, Professor Michael Timko, from Worcester Polytechnic Institute for giving me the opportunity to work with his team. I would also like to thank my mentor, PhD candidate Ziyang Zhang, for his time, guidance, and support.

Chapter 1: Introduction

The rising levels of greenhouse gas emissions is a concern due to the continual increase in land and ocean temperatures at an average rate of .13°F per decade (Lindsey, Dahlman 2021). Figure 1.1 shows the changes in global average surface temperature from 1990 to 2019 (NOAA 2021). Places that have warmed up to 1°F over the past 30 years is marked in red. While places that have cooled up to 1°F are marked in blue. The trends show a majority of land and oceans increasing in surface temperature.

Levels of the two most important anthropogenic greenhouse gases, carbon dioxide and methane, continue to rise contributing to global average temperature increase (Stein 2021). This is due to the heavy reliance of fossil fuels as a primary energy source for transportation, electricity, and industry sectors. Climate Change mitigation strategies involve reducing carbon emissions by adopting renewable energy sources, such as solar, wind, hydro, and biomass (Elum, Momodu 2017). However, fossil fuels still account for nearly 80% of the total energy consumed in the United States (EIA 2021).

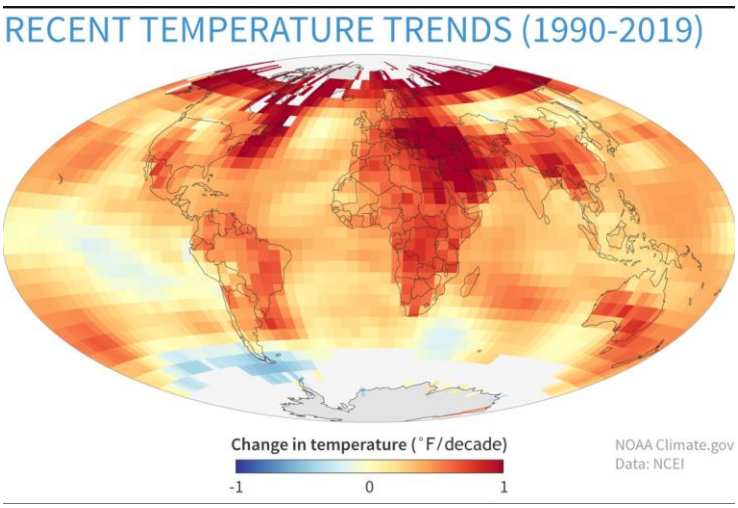

Figure 1.1: Changes in global average surface temperature from 1990-2019. Places warmed up to 1°F over the past 30 years in red, places cooled up to 1°F in blue. NOAA Climate.gov, based on NCEI data

Another contributing factor to rising GHG emissions stem from food waste ending up in landfills. Landfill gas emissions are one of the largest anthropogenic sources of methane largely due to food waste decomposition (Adhikari 2006), accounting for about 9% of global greenhouse gas emissions. A method to combat both food waste and provide an alternative energy source is biomass.

Biomass can include wood, agricultural crops and waste materials, municipal solid waste, plant waste, food waste, ect. (Anon 2020). Using biomass to create biofuels would provide a net zero greenhouse gas emission alternative to fossil fuels and reduce the quantity of food waste in landfills that contribute to rising methane levels. According to the analysis by the United National Conference on Environment and Development, biomass will potentially supply about half of the world primary energy consumption by the year 2050 (Yu et al 2008).

Biomass captures and converts solar energy into chemical energy as carbohydrates through photosynthesis reactions of carbon dioxide and water (Yu et al 2008). These biomass carbohydrates mainly consist of cellulose and hemicellulose. A process called hydrolysis breaks down the cellulose to extract sugars that can then be used to produce ethanol.

The current hydrolysis model consists of a mechanical pretreatment of the cellulose to create amorphous cellulose. The amorphous cellulose is placed with water and a catalyst, such as hydrochloric acid, at a high temperature to produce glucose. However, when the amorphous cellulose comes in contact with water during the hydrolysis process, the hydrogen bonds reactivate, causing the cellulose structure to recrystallize. The recrystallization of cellulose is undesired, as it prevents the continuous breakdown of the bonds that would produce glucose. This limits the full potential of the biomass to be further processed into biofuel.

A proposed solution is to add salts to the hydrolysis process to suppress cellulose recrystallization, allowing for further glucose production. There are numerous literatures reporting the use of salts during cellulose hydrolysis,however, there is currently no comprehensive study revealing how the salts effect the cellulose structure.

The goal of this project was to show that chaotropic salts, such as guanidinium chloride, will suppress cellulose recrystallization, thus leading to higher glucose yields, while kosmotropic salts, such as ammonium chloride, will stabilize the water structure, thus leading to lower glucose yields.

Chapter 2: Background

2.1 Lignocellulosic Biomass -Structure and Composition

The difficulty of converting lignocellulose to commercial products are routed in its complex chemical structure (Tyufekchiev 2019). Lignocellulose Biomass refers to plant biomass that is composed of three main polymers: cellulose, hemicellulose, and lignin. A typical arrangement can be seen in figure 2.1. The three polymers link together through a complex structure, called a cell wall. The cell wall provides structural support and protection against biological and chemical agents (Rubin 2008). Cellulose, consisting up to 35-55% weight of the structural component, is comprised of long glucose chains held together by glycosidic bonds and hydrogen bonds. Hemicellulose consists of a family of polysaccharides linking cellulose fibers into microfibrils and crosslinks with lignin, giving the structural strength to the cell walls (Rubin 2008). Lignin is a polymer of phenylpropanoid units and provides the cell wall with stiffness through compressive forces, which can be considered the glue that holds it all together.

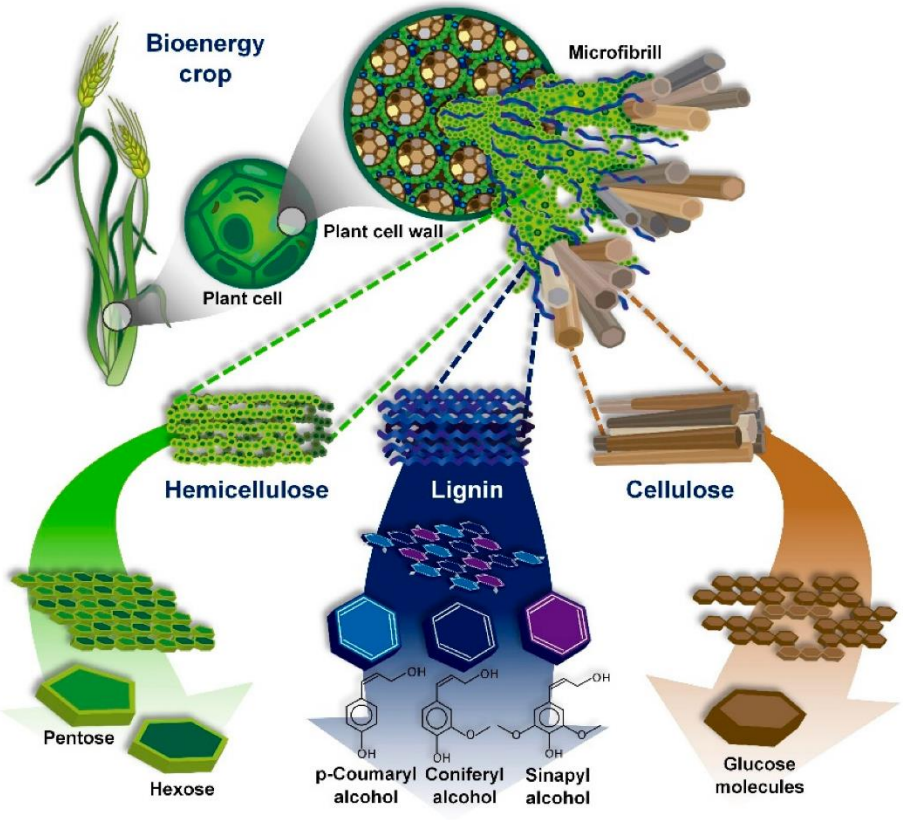

Figure 2.1 Typical arrangement of Lignocellulose (Hernández-Beltrán et al 2019)

2.2Cellulose

Cellulose is a homopolymer consisting of repeating linear glucose units held together by β 1–4 glycosidic bonds. These linear, unbranched chains interact with one another through van der Waal forces and hydrogen bonding, giving cellulose a highly organized crystalline structure (O'sullivan 1997). The β 1–4 glycosidic bond refers to the bond formed between the carbon-1 of one monosaccharide and the carbon-4 of the neighboring monosaccharide. Figure 2.2 shows a representation of the composition and structure of cellulose.

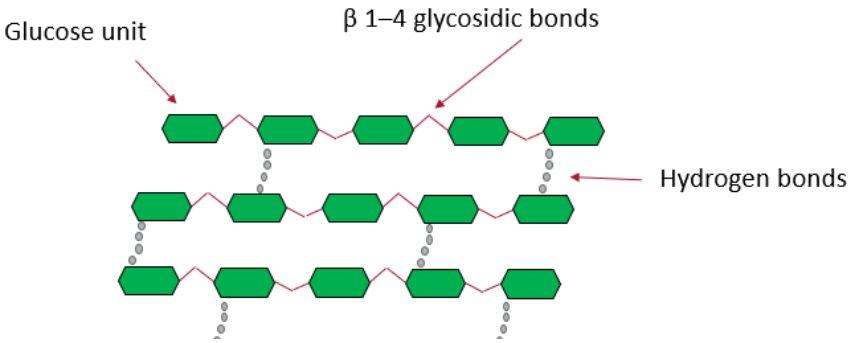

Figure 2.2: Representation of Cellulose Structure: Highly Crystalline Structure through Beta1,4 glycosidic bonds, van der Waal Forces, and Hydrogen Bonding

2.3 Current Cellulose Hydrolysis Model

The purpose of hydrolysis is to break the glycosidic bonds that link the sugar monomers together. Hydrolysis is typically carried out at temperature below 300°C with either dilute acid or no acid. These conditions maintain cellulose in its solid state and does not undergo a phase change. The sugar monomers can be further processed to become ethanol. The rate of cellulose hydrolysis to glucose monomers can be increased either by an increase in temperature or using a homogeneous acid as a catalyst.

The current cellulose hydrolysis model consists of breaking the hydrogen bonds through a mechanical pretreatment, such as ball milling. This process breaks the hydrogen bonds and creates an amorphous structure. The amorphous cellulose is then exposed to water at a certain temperature (with or without dilute acid) and duration to break the glycosidic bonds to form glucose. However, evidence points to water-induced cellulose-recrystallization, preventing the continued breakdown of the glycosidic bonds.

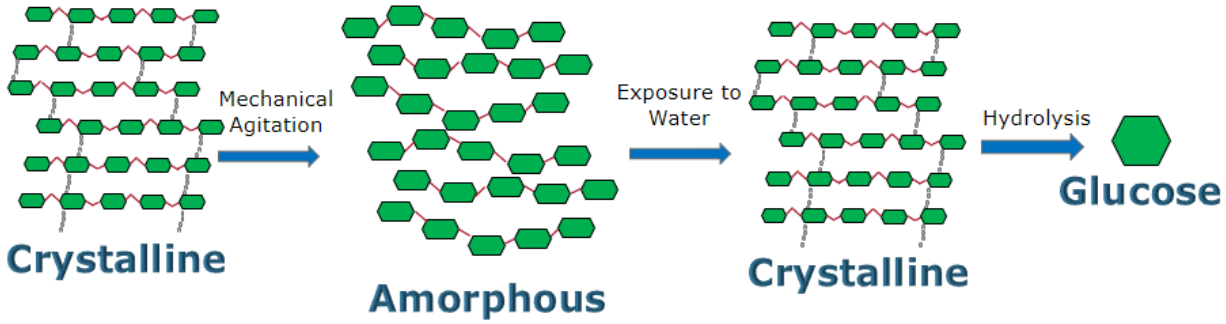

Figure 2.3 model of cellulose hydrolysis

In our study, we perform dilute acid hydrothermal hydrolysis of cellulose. We use a concentration of .05M HCl as a catalyst and perform the hydrolysis at 150C.

2.4 Hofmeister Series

In 1888, Franz Hofmeister first reported the salts to precipitating proteins and macromolecules out of aqueous solution generally follow a specific ion series and were ranked accordingly by physical behaviors (Zhang and Cremer 2006). The Hoffmeister series provides a qualitative ranking of ions with respect to their ability to solubilize or aggregate the proteins in a solution. The series is centered around chloride and sodium, known as a reference of "neutral" effects within each of the series (Wicky et al 2017). In this series, Chaotropic salts improve protein solubility (salting-in), while kosmotropic salts decrease (salting-out) protein solubility.

Although this series was used for the effects on protein stability, cellulose has a similarity to protein, as they are both amphipathic. This means that both cellulose and proteins contain hydrophobic groups and hydrophilic groups. Proteins have hydrophilic groups, such as glycine or alanine, and hydrophobic groups, such as serine or threonine. Similarly, cellulose contains a hydrophilic group, -OH, and hydrophobic groups, -C-O-C-CH_2 and -CH_3. A visual of these portions for cellulose can be seen in figure 2.5.

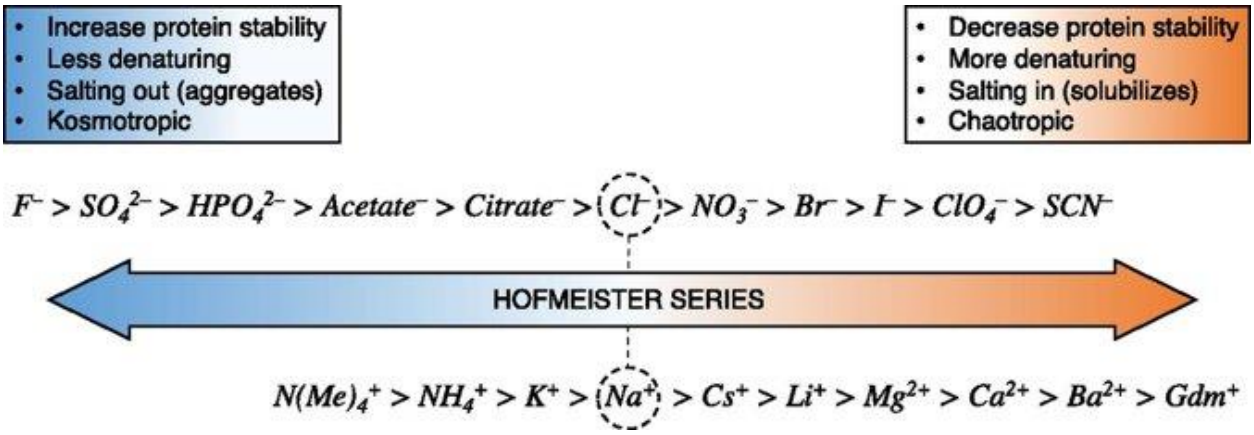

Figure 2.4 Hofmeister Series Salt Selections for both anions and cations. (Wicky et al 2017)

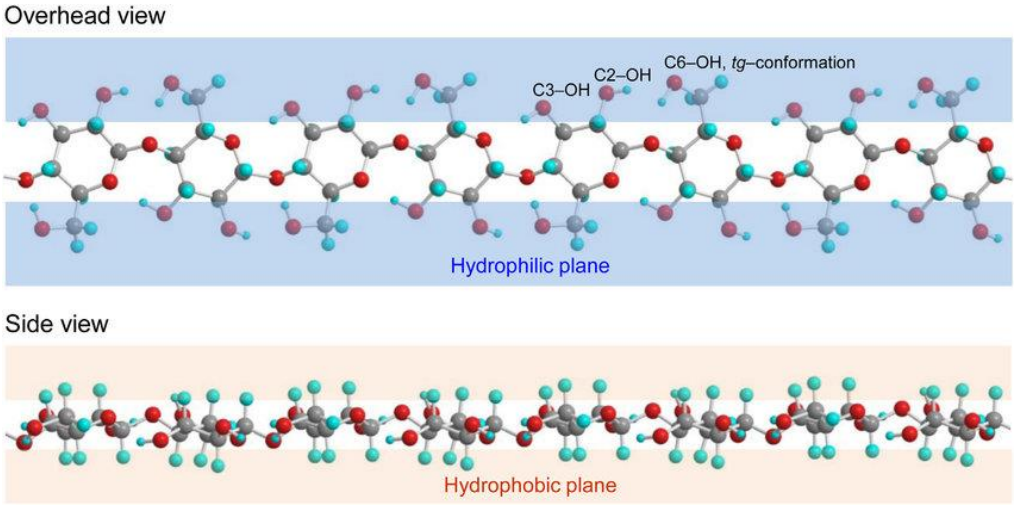

Figure 2.5 Amphipathic portions of Cellulose model (Isogai et al 2018)

Because proteins and cellulose have this similarity, we believe the Hofmeister series can be applied to cellulose hydrolysis as well. We selected salts based off the Hofmeister series with the hypothesis that chaotropic salts, such as guanidinium chloride will suppress water-induced cellulose-recrystallization leading to higher glucose yields, while kosmotropic salts, such as ammonium chloride, will stabilize the water structure not effecting glucose yields.

Chapter 3: Methodology

Materials and Methods

3.1Materials

Microcrystalline cellulose (Avicel PH-101, 50µm particle size, Fluka Analytical), HCl, Na_2CO_3, NaOH, NaCl, NaH_2PO_4, $NaNO_3$, GdmCl, $CaCl_2$, KCl, NH_4Cl, HCl

3.2Methods

3.2.1 Ball milling Pretreatment

Figure 3.2.1 shows a representation of the setup. 2 5-mm diameter stainless steel balls were placed in the stainless-steel ball-milling vessel, separated by one 10mm diameter stainless steel ball. Next, 1 gram of microcrystalline cellulose was placed over the stainless-steel balls. The vessel was sealed with a rubber O-ring between the lid and the vessel, then wrapped with insulating tape to prevent leakage during the ball milling process. The prepared vessel was loaded into the ball-milling machine and tightened into place. The sample was milled for 50 minutes at a frequency of 60 Hertz. This method uses the vibratory ball mill processes. In vibratory mills, the vessel containing the sample and grinding medium are shaken back and forth at high vibrational frequencies (Piras et al. 2019).

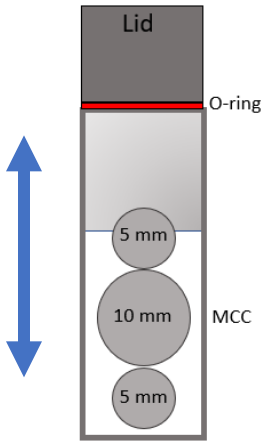

Figure 3.2.1: Schematic ball-mill vessel setup

3.2.2 Oil Bath Temperature Calibration

An Optichem heat and stirrer plate was used in the experiments. The setup for all of the experimental runs had three test tube clamps set equally distant from the center of the silicone oil bath and at the same heights. The target internal sample temperature was 150C. The final setting temperature for the oil bath was 173C. The calibration was performed by using a k-type thermocouple that had been modified onto a pressurized cap. 2mL of .05M HCl was used in the vessel as a volume control. The modified thermocouple vessel was place at equal heights above the oil bath, such that the liquid was fully submerged below the oil. Figure 3.2.2 shows a layout of the setup. A time study was performed on the liquid as it heated to the set temperature. This was repeated for each location to be used in the oil bath to ensure proper temperature had been reached. As stated, 173C was the final temperature setting for the Optichem heat plate for an internal temperature of 150C to be reached. The data from this calibration was used to include a 10-minute warmup time to ensure the temperature of the sample was at 150C for the entirety of the time desired.

Figure 3.2.2: Temperature Calibration setup

3.2.3 Preparing Salt Solutions

A 1M concentration of each salt was desired for the experiments. The equation $M = \frac{n}{V}$, where M is the molarity, n is the number of moles, and V is the volume in liters, was used to solve for the number of moles. This information was used with the molar mass of the salt to solve for the needed mass for a volume of 40mL. For this section, we used Excel to calculate the needed mass of each salt. A sample calculation for desired mass can be viewed in the Appendix.

3.2.4 Salt-Acid Hydrolysis

.1 grams of 50-minute ball milled MCC was subject to a hydrothermal treatment at 150C for various time frames, in different aqueous salt solutions of .5M ionic strength and .05M ionic strength HCl catalyst. As a control, the same molar concentrations were used for all experiments. To prepare the vessel, 1mL of 1M salt solution was added to the vessel and 1mL of .1M HCl solution was added to the vessel. The experiments were run in triplets using the same setup as the oil bath temperature calibration. The reaction temperature was controlled at 150C in an oil bath and the stir bar mixing speed was set at 200 rpm. Figure 3.2.4 shows the oil bath set up of the samples. The reaction times were fixed at 1 hour and 4 hours to include a 10-minute warmup. The 10-minute warmup allowed for the liquid inside the vessels to reach 150C. The hydrolysis was stopped by submerging the vessels in ice once the desired time was reached. The samples were then subjected to a centrifuge process described in the next section.

Figure 3.2.4: Oil bath Hydrolysis Setup

3.2.5 Centrifuge Process and Sample Collection

A Thermo Scientific Sorvall Legend RT+ Centrifuge was used to separate the liquid from the solid. The following settings were used for each of the samples. The ramp up and ramp down speed was set to 5. The rpm was set to 3000 rpm. The time was set to 10 minutes. The temperature was set to 25C. The samples were loaded into the centrifuge and ran for 10 minutes. The liquid was extracted from the vial and saved for analysis. The solid was washed with 2mL of acetone and shaken to ensure even washing of the solid. The vial was placed in the centrifuge for 10 more minutes. The liquid was extracted and removed to the proper waste. 2mL of acetone was added to the sample again and shaken to ensure even washing. The vial was placed in the centrifuge for a final 10 minutes. The liquid was extracted and disposed of in

the proper waste. The solid was then placed into a 60C oven to dry overnight. Figure 3.2.5 shows the centrifuge used for the process.

Figure 3.2.5: Images of Centrifuge setup

3.3 Characterization

3.3.1 X-Ray Diffractometer (XRD)

X-Ray Diffractometer, also known as XRD, was a technique used to measure the crystallinity of the cellulose using a Rigaku Geigerflex diffractometer. Cu Kα radiation was emitted at 37.5kV and 25mA. A step size of 0.05° was used with 1 second accumulation time. Diffractograms of the different samples were compared after the area was normalized and baseline subtraction. Crystallinity of the cellulose was calculated by using the peak height method, a method developed by Segal (Segal et al. 1959). This method takes height ratio between the intensity of the crystalline peak and the total intensity after the subtraction of the non-crystalline signal. The following equation was used:

$$CI(\%) = \frac{I_{200} - I_A}{I_{200}} X\ 100\%$$

CI is the calculated crystallinity in percent (%), I_{200} is the maximum intensity of the peak that corresponding to the plane with the Miller indices 200 at the 2Θ angle at 22.5°. I_A is the intensity of diffraction of the background scatter (amorphous), at the 2Θ angle of about 18.3° in the valley between the peaks (Terinte et al. 2011). Figure 5 shows the XRD results for raw MCC and the 50-minute ball-milled MCC. The highest peak, marked with the 200 Miller indices, is the highly crystalline portion of cellulose I. The peak is drastically reduced after the 50-minute ball milling. From this observation, we can see that the post process of ball milling greatly increases the amorphous regions in cellulose I.

3.3.2 High Performance Liquid Chromatography (HPLC)

Liquid products were analyzed with High Performance Liquid Chromatography (HPLC, Shimadzu LC-40 model). A diode array detector (DAD) was used for organic acids and furanic compounds and a refractive index detector (RID) for carbohydrate detection. Bio-Rad Aminex HPX-87H (Phenomenex) was used for product separation. The mobile phase was 5 mM sulfuric acid for preventing bacteria growing. The mobile phase flow rate was 0.6 mL/min and analyzing temperature was 35 °C. A series of standard glucose solutions was prepared for obtaining calibration curve, which are 0.25, 0.5, 1, 2 and 5 g/L.

Chapter 4: Results and Discussion

4.1 Cation Effect on Suppression of Cellulose Recrystallization

We determined if our salt selections had an effect of suppressing cellulose recrystallization. This was performed with the 50-minute ball-milled cellulose with .5M aqueous salt solution at 150C for 2-hours. In all the aqueous salt solutions, the 200_cellulose plane and the 110_cellulose plane recrystallized, but at different kinetic speeds, marked as “200” and “110 on the XRD chart below in figure 4.1. After the 2-hour duration, the sample with no salt (water) caused cellulose to restore its crystallinity completely. Guanidinium Chloride suppressed cellulose recrystallization the most, followed by Calcium Chloride, Potassium Chloride, Lithium Chloride, and Ammonium Chloride, respectively.

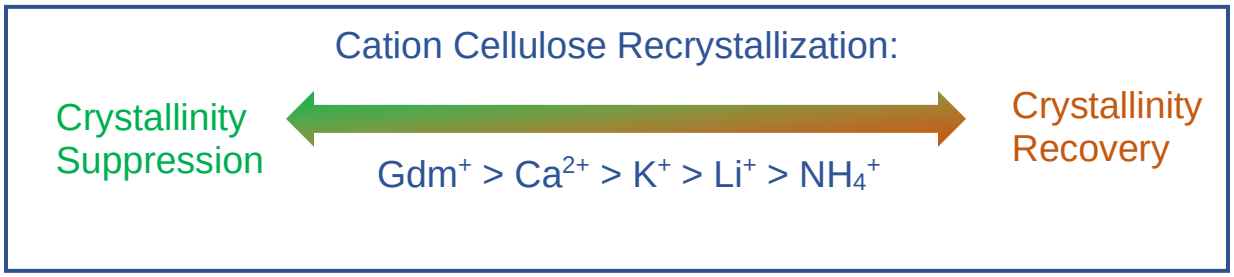

It is noted that the suppression of recrystallization was mainly from the cations in the salt, since we fixed the anion in all samples as chloride. The Segal crystallinity index calculations, shown in table 4.1, show that chaotropic salts, such as guanidinium chloride, suppressed the cellulose recrystallization the most and kosmotropic salts, such as ammonium chloride, suppressed cellulose recrystallization the least.

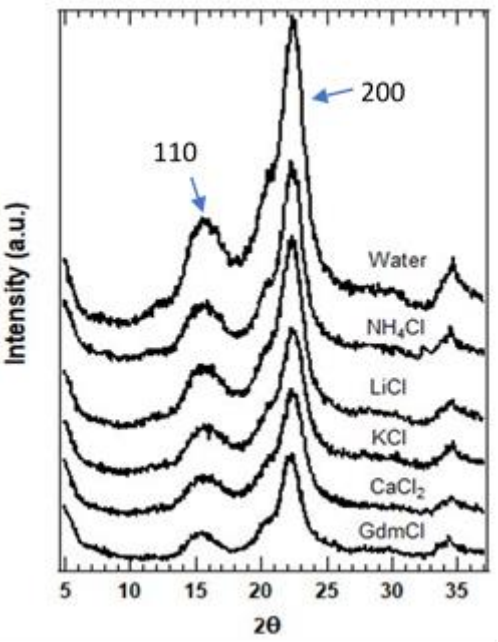

Figure 4.1: XRD results of 2-hour,150C Fixed-Anion Salt Selections

Table 4.1: Segal Crystallinity Indexes for Fixed-Anion Salt Selection

Sample	Segal Crystallinity Index (%)
Water	88.2 %
NH_4Cl	86.6 ± 1.1 %
LiCl	80.1 ± 2.2 %
KCl	81.1 ± 1.8 %
$CaCl_2$	78.9 ± 1.0 %
GdmCl	79.1 ± 2.1 %

4.2 Anion Effect on Suppression of Cellulose Recrystallization

Similar experiments were performed to see if anions influenced the suppression of cellulose recrystallization. This was performed with the 50-minute ball-milled cellulose with .5M aqueous salt solution at 150C for 1-hour. In all the aqueous salt solutions, the 200_cellulose plane and the 110_cellulose plane recrystallized, but at different kinetic speeds, marked as “200” and “110 on the XRD chart below in figure 4.2. After the 1-hour duration, the sample with no salt (water) caused cellulose to restore its crystallinity completely. Sodium Hydroxide suppressed cellulose recrystallization the most, followed by Sodium Phosphate, Sodium Chloride, Sodium Acetate, and Sodium Carbonate, respectively. Sodium Carbonate and Sodium Acetate fully restored cellulose crystallinity post heat treatment and did not influence suppressing cellulose recrystallization.

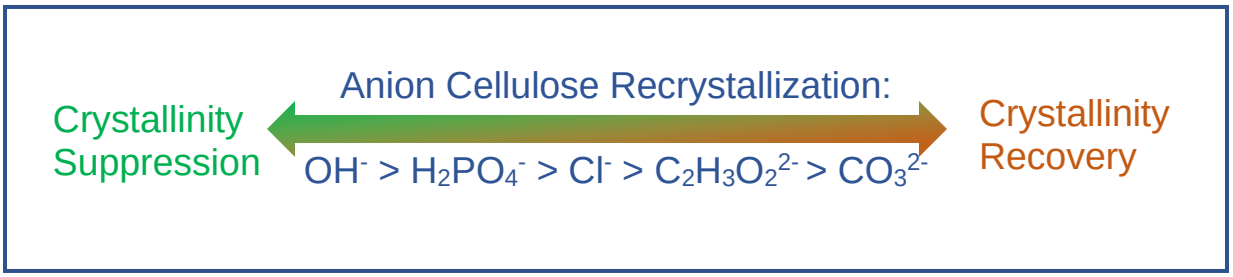

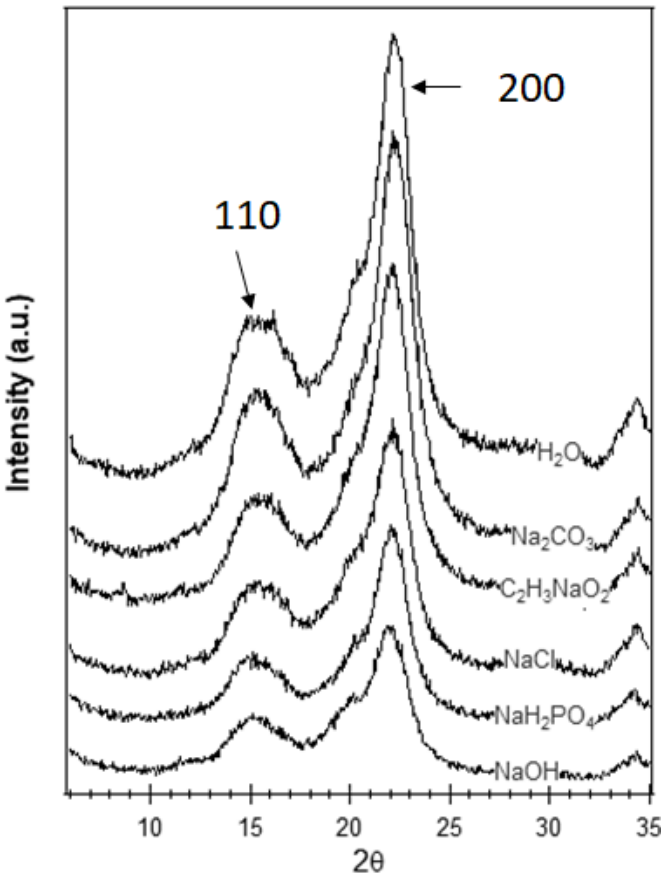

Figure 4.2: XRD results of 1-hour,150C Fixed-Cation Salt Selections

Table 4.2: Segal Crystallinity Indexes for Fixed-Cation Salt Selection

Sample	Segal Crystallinity Index (%)
Water	91.86 %
Na_2CO_3	91.85 %
$C_2H_3NaO_2$	91.64 %
NaCl	90.91 %
NaH_2PO_4	88.11 %
NaOH	89.02 %

4.3 Glucose Yields of Fixed-Anion Salt Selections

.1 grams of 50-minute Ball-milled MCC was added with .5M aqueous salt solution and .05M HCl at 150C for 4 hours. The liquid was analyzed by HPLC to determine the glucose yields. Figure 4.3 shows the yield results. Adding salts increased the glucose yield. Without any salt, Hydrochloric Acid only produced 23% glucose yield (no-salt). Guanidinium chloride produced the highest glucose yield with around 37%. Calcium Chloride produced around 31%, Potassium Chloride produced around 27.5%, Lithium Chloride produced around 26.5%, and Ammonium Chloride produced around 23%. The results of the glucose yields agree with the recrystallization suppressing performance.

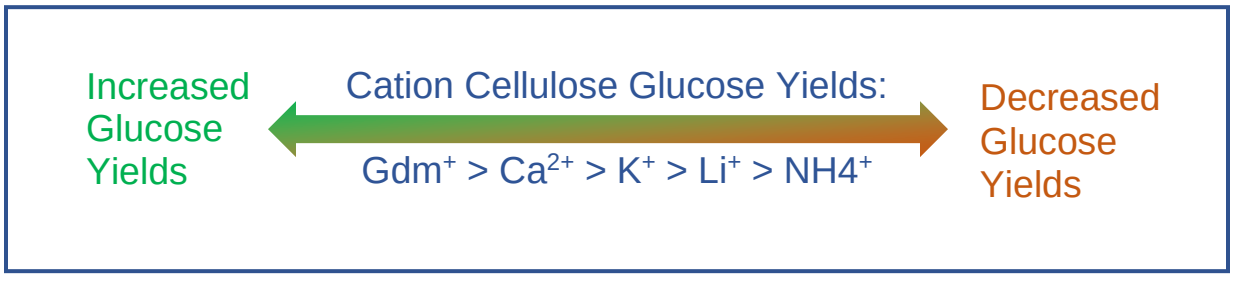

HPLC was also performed on the salt selections that were ran for 2 hours with no acid. As expected, no glucose was produced. This indicates that the increase of glucose yield post hydrolysis is due to the salts ability to suppress the cellulose recrystallization.

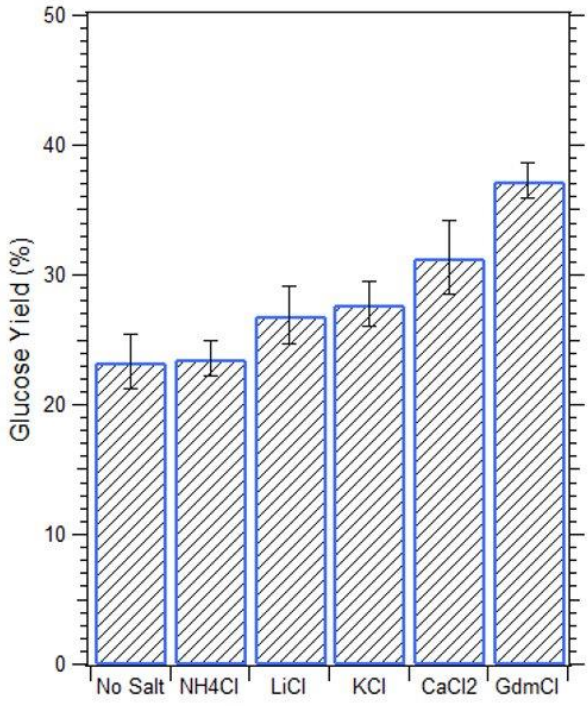

Figure 4.3: Glucose yields of 50-minute Ball-Milled Cellulose in HCl and Fixed-Anion Salts

4.4 Glucose Yields of Fixed-Cation Salt Selections

The same technique was used to acquire the glucose yields for the fixed-cation salts. Figure 4.4.1 shows the glucose yield results. Sodium Chloride produced the highest glucose yields with around 25%. Sodium Hydroxide produced a glucose yield of about 6%. Sodium carbonate, sodium phosphate, and sodium acetate produced glucose yields of less than 1%. The results of the fixed-cation data showed that the anions from the various salt selections possibly had a reaction with the acid. XRD was performed on these samples to see if the recrystallization supported that possibility.

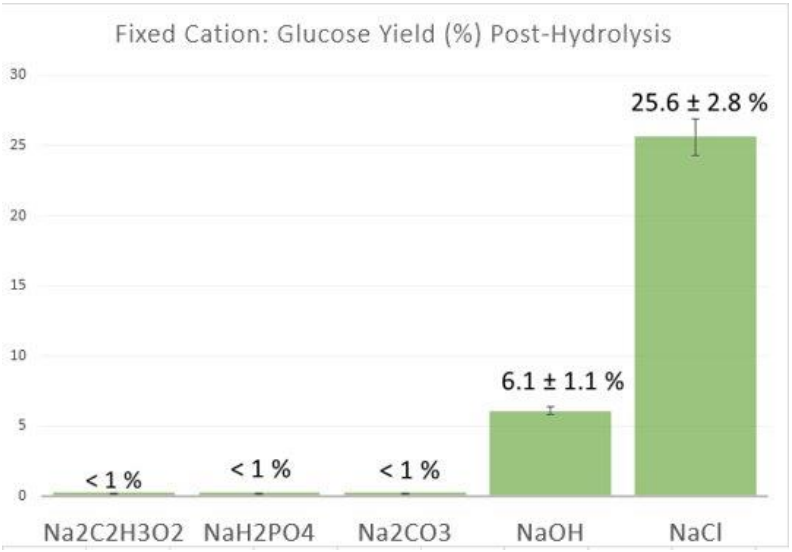

Figure 4.4.1: Glucose yields of 50-minute Ball-Milled Cellulose in HCl and Fixed-Cation Salts at 150C for 4 hours

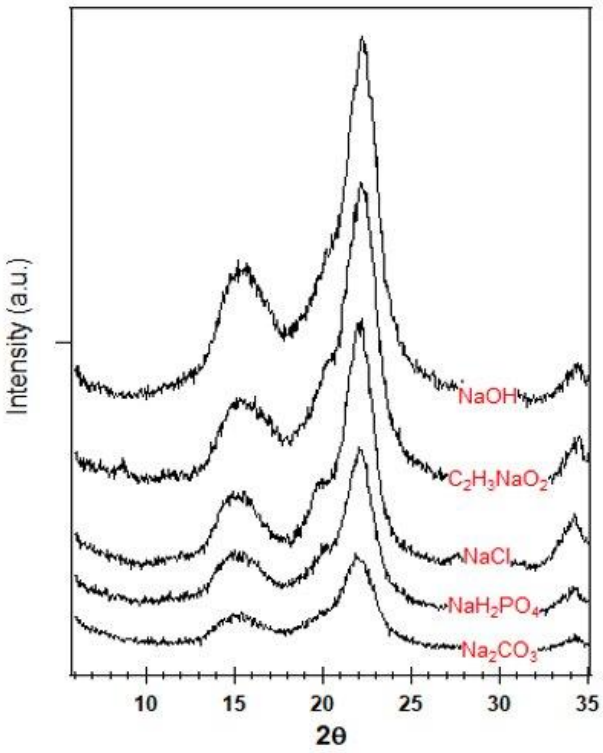

Figure 4.4.2: XRD data of Fixed-Cation salts Post Hydrolysis

Post hydrolysis, sodium hydroxide suppressed cellulose recrystallization the least, while sodium carbonate suppressed cellulose recrystallization the most. The difference in the XRD results, as seen in figure 4.4.2, show that some of the salt interacted with the acid during hydrolysis, limiting the amount of salt to suppress crystallinity.

Table: Acid-Base Reactions	*pKa*	*Glucose Yields (%)*
$NaCl + HCl \rightarrow NaCl + HCl$ Strong Acid: $HCl + H_2O \rightarrow H_3O^+ + Cl^-$	-9.3	25.6%
$NaOH + HCl \rightarrow NaCl + H_2O$	14.0	6.1%
$Na_2CO_3 + 2HCl \rightarrow 2NaCl + H_2CO_3$ $H_2CO_3 + H_2O \rightarrow HCO_3^- + H_3O^+$ $HCO_3^- + H_2O \rightarrow CO_3^- + H_3O^+$	6.37: 10.329	<1%
$CH_3COONa + HCl \rightarrow NaCl + CH_3COOH$ Weak acid: $CH_3COOH + H_2O \leftrightarrow CH_3COO^- + H^+$	4.75	<1%
$NaH_2PO_4 + 2HCl \rightarrow NaHCl_2 + H_3PO_4$	2.12	<1%

The pKa value of the acid produced from the salt-acid interaction for each sample shows how tightly the proton is held by a Brønsted acid. The lower the pKa of a Brønsted acid, the more easily it will give up its proton. Likewise, the higher the pKa of a Brønsted acid, the tighter the proton is held. Sodium chloride produced a glucose yield of 25.6%. Hydrochloric acid has a pKa value of -9.3, making it a strong acid. This acid fully disassociates in water, creating a proton and a chlorine anion. The proton can continue to attack the glycosidic bonds to produce more glucose units. On the other hand, if the Brønsted acid has a larger value, such as those of carbonic acid (6.37) and acetic acid (4.75), then the proton is held on tighter and cannot attack the cellulose to produce glucose, resulting in less than 1 % production.

Chapter 5: Conclusion

The salts' ability to suppress crystallinity correlates with its performance in glucose yield, showing that the performance of salts agrees with the Hofmeister series. The XRD data supported the hypothesis that salting-in salts, such as Guanidinium Chloride, would suppress cellulose recrystallization, while salting-out salts, such as Ammonium Chloride, would support cellulose recrystallization. Guanidinium Chloride produced the highest glucose yields after hydrolysis, while ammonium chloride produced the least amount of glucose for the fixed-anion salt selections.

Although Sodium hydroxide suppressed cellulose crystallinity the most, it produced only 6% glucose due to the salt-acid interaction during hydrolysis. Sodium Chloride performed best of the fixed-cation salts due to its minimal salt-acid interaction.

The best performing salt overall was Guanidinium Chloride. A further study is continued to examine the molecular dynamics of the cation's interaction with the cellulose hydrophobic and hydrophilic groups.

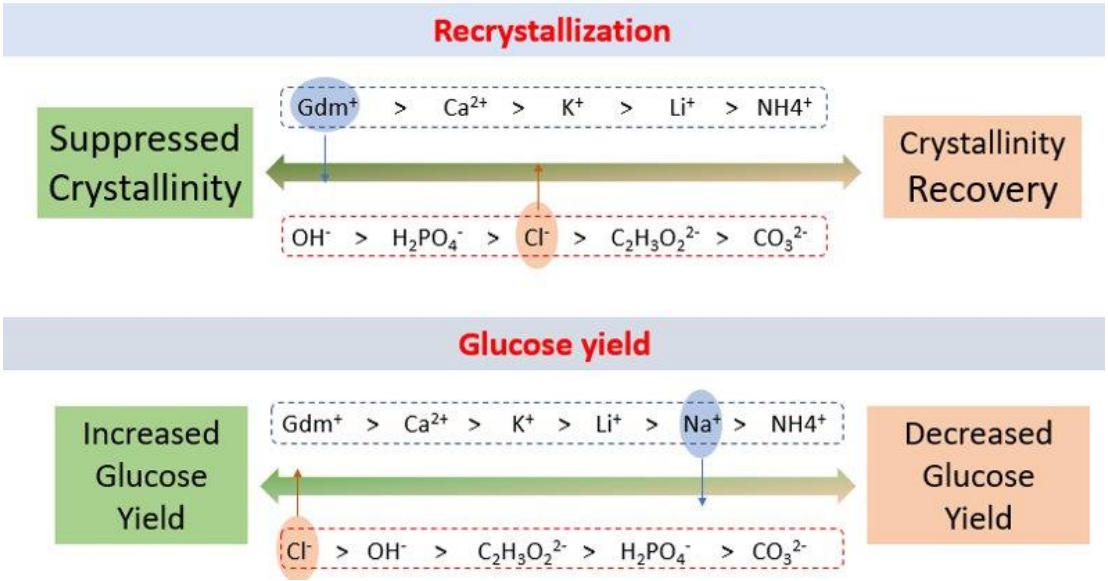

References

Piras, C.C., Fernández-Prieto, S. and De Borggraeve, W.M., 2019. Ball milling: a green technology for the preparation and functionalisation of nanocellulose derivatives. Nanoscale Advances, 1(3), pp.937-947.

Terinte, N., Ibbett, R. and Schuster, K.C., 2011. Overview on native cellulose and microcrystalline cellulose I structure studied by X-ray diffraction (WAXD): Comparison between measurement techniques. *Lenzinger Berichte*, *89*(1), pp.118-131.

Segal L, Creely JJ, Martin AE, Conrad CM (1959) An empirical method for estimating the degree of crystallinity of native cellulose using the X-Ray diffractometer. Text Res J 29(10):786–794. doi:https://doi.org/10.1177/004051755902901003

Stein, T., 2021. Despite pandemic shutdowns, carbon dioxide and methane surged in 2020. Welcome to NOAA Research. Available at: https://research.noaa.gov/article/ArtMID/587/ArticleID/2742/Despite-pandemic-shutdowns-carbon-dioxide-and-methane-surged-in-2020 [.

Ritchie, H., Food waste is responsible for 6% of global greenhouse gas emissions. *Our World in Data*. 2020 Available at: https://ourworldindata.org/food-waste-emissions.

Lindsey, R. & Dahlman, L.A., 2021. Climate Change: Global Temperature: NOAA Climate.gov. *Climate Change: Global Temperature | NOAA Climate.gov*. Available at: https://www.climate.gov/news-features/understanding-climate/climate-change-global-temperature#:~:text=According%20to%20NOAA's%202020%20Annual,more%20than%20twice%20that%20rate. [Accessed May 2, 2021].

Elum, Z.A. and Momodu, A.S., 2017. Climate change mitigation and renewable energy for sustainable development in Nigeria: A discourse approach. *Renewable and Sustainable Energy Reviews*, *76*, pp.72-80.

Adhikari, B.K., Barrington, S. and Martinez, J., 2006. Predicted growth of world urban food waste and methane production. *Waste Management & Research*, *24*(5), pp.421-433.

Chen, H., 2014. Chemical composition and structure of natural lignocellulose. In *Biotechnology of lignocellulose* (pp. 25-71). Springer, Dordrecht.

Anon, 2020. U.S. Energy Information Administration - EIA - Independent Statistics and Analysis. *Biomass explained - U.S. Energy Information Administration (EIA)*. Available at: https://www.eia.gov/energyexplained/biomass/#:~:text=Direct%20combustion%20is%20the%20most,biomass%20includes%20pyrolysis%20and%20gasification. [Accessed May 2, 2021].

Bolye, G., Ed.; Renewable Energy—Power for a Sustainable Future; Oxford University Press: Oxford, U.K., 1996

Yu, Y., Lou, X. and Wu, H., 2008. Some recent advances in hydrolysis of biomass in hot-compressed water and its comparisons with other hydrolysis methods. *Energy & fuels*, *22*(1), pp.46-60.

Hernández-Beltrán, J.U., Lira, H.D., Omar, I., Cruz-Santos, M.M., Saucedo-Luevanos, A., Hernández-Terán, F. and Balagurusamy, N., 2019. Insight into pretreatment methods of lignocellulosic biomass to increase biogas yield: current state, challenges, and opportunities. *Applied Sciences*, *9*(18), p.3721.

Tyufekchiev, M.V., 2019. *Reaction Engineering Implications of Using Water for the Conversion of Lignocellulosic Biomass* (Doctoral dissertation, Worcester Polytechnic Institute).

Rubin, E.M., 2008. Genomics of cellulosic biofuels. *Nature*, *454*(7206), pp.841-845.

O'sullivan, A.C., 1997. Cellulose: the structure slowly unravels. *Cellulose*, *4*(3), pp.173-207.

Zhang, Y. and Cremer, P.S., 2006. Interactions between macromolecules and ions: the Hofmeister series. *Current opinion in chemical biology*, *10*(6), pp.658-663.

Wicky, B.I., Shammas, S.L. and Clarke, J., 2017. Affinity of IDPs to their targets is modulated by ion-specific changes in kinetics and residual structure. *Proceedings of the National Academy of Sciences*, *114*(37), pp.9882-9887.

Isogai, A., Hänninen, T., Fujisawa, S. and Saito, T., 2018. Catalytic oxidation of cellulose with nitroxyl radicals under aqueous conditions. *Progress in Polymer Science*, *86*, pp.122-148.

Procedures Addendum:

Salt solution prep:

1. Calculate the mass of salt needed for desired molarity. The information needed is the molar mass of the salt (g/mol), the desired molarity concentration , and the volume of solution (L).
2. Measure the mass of solid needed
3. Pour salt into vial. Fill with distilled water to the desired volume
4. Place cap on vial and shake until salt is dissolved

Ball-mill sample prep:

1. Prepare the ball mill vessel for use. Ensure the vessel and balls are clean. Place the stainless-steel balls in small, large, small order.
2. Measure and place 1 gram of Avicel in each ball mill vessel
3. Place o-ring and cover on each vessel. I use electrical tape to ensure the cover does not come off during the ball milling process
4. Place each of the prepared vessels into the ball mill machine.
5. Power on the machine and set the timer for 50 minutes
6. The unit will stop itself once the desired time has elapsed
7. Caution; the vessels will be hot to the touch when removing them from the machine post-process.

Experimental procedure

1. Preheat oil bath to 173C. turn stirrer onto 200 rpm
2. Prepare 3 identical samples using heavy wall cylindrical bottom pressure vessels
    a. Place a stir bar into the glass vessel
    b. Measure and place .1 grams of 50-minute ball milled cellulose into vessel
    c. Measure 1 mL of prepared salt solution and place into vessel
    d. Measure 1 mL of prepared catalyst solution and place into vessel
    e. Place cap on tightly
    f. Repeat steps a-e for the other two samples
3. Once the oil bath has reached set temperature, place the prepared samples in the tube clamps. Ensure the prepared samples are submerged at the same depth as during calibration.
4. Set a timer for the desired duration, to include a ten minute warm up for the sample
5. Have ice on standby to quickly cool the samples once the time has elapsed.
6. Ice the samples for about 10-15 minutes until the samples are cooled.
7. Wipe off excess oil from the exterior of the glass vessels
8. Transfer the samples to clean plastic centrifuge tubes
9. Centrifuge the samples for 10 minutes
10. Extract the liquid from the sample and save for analysis
11. Perform an acetone wash
    a. Place 2mL of acetone into the sample.
    b. Replace lid and shake vigorously
12. Centrifuge sample for 10 more minutes
13. Extract the liquid and discard into proper hazardous waste receptacle
14. Repeat steps 11-13 once.
15. Place the solid sample in a oven and dry over night (60C)
16. Save solid for analysis

Centrifuge steps

1. Turn on power supply to centrifuge (Thermo Scientific Sorvall Legend RT+ Centrifuge)
2. Set the ramp up and ramp down to 5
3. Set the rpm to 3000
4. Set the time to 10
5. Set the temperature to 25
6. Press the open lid symbol to open centrifuge
7. Load in samples. Ensure the load is balanced or else extreme cavitation will occur
8. Press the start button
9. When time is complete, sample will ramp down in speed and will machine will beep when ready.
10. Press the same button as in step 6 to open machine.

11. Remove samples
12. Power off device when finished

Sample Calculations to determine mass for molar solution preparation

Determine mass required to prepare molar solution.

Example: 40mL of a 1M solution of NaCl

$M = \frac{n}{V}$: M-molarity, n-moles, V-volume (L)

Molar mass NaCl: 58.44 grams/mol

Molarity: 1 M or 1 mol/L

Volume 40 mL or .04L

Solve for n: n=1M*.04L = .04mol

Solve for grams: molar mass*n

(58.44g/mol)*(.04moles) = 2.3376 grams